Nanoscale

Crumpled Graphene Balls-based Broadband Solar Absorber

Journal:	*Nanoscale*
Manuscript ID	NR-COM-12-2017-009556.R1
Article Type:	Communication
Date Submitted by the Author:	04-Feb-2018

Complete List of Authors:	Hao, Wei; Shanghai Jiao Tong University, Materials Science and Engineering Chiou, Kevin; Northwestern University, Materials Science and Engineering Qiao, Yiming; Shanghai Jiao Tong University, Materials Science and Engineering Liu, Yanming; Shanghai Jiao Tong University, Materials Science and Engineering Song, Chengyi; Shanghai Jiao Tong University, School of Materials Science and Engineering Deng, Tao; Shanghai Jiao Tong University, materials science and engineering Huang, Jiaxing; Northwestern University, Materials Science and Engineering

Journal Name

COMMUNICATION

Crumpled Graphene Balls-based Broadband Solar Absorber

Wei Hao,[a,b] Kevin Chiou,[b] Yiming Qiao,[a] Yanming Liu,[a] Chengyi Song,[a] Tao Deng*[a] and Jiaxing Huang*[b]

Received 00th January 20xx,
Accepted 00th January 20xx

DOI: 10.1039/x0xx00000x

www.rsc.org/

Sheet-like graphene tends to stack with each other in thin films, resulting in relatively smooth microstructures with increased reflection as the thickness increases. In contrast, when the sheets are crumpled into a shape like paper balls, reflection is greatly reduced. In this work, crumpled graphene balls are found to be strong light absorbers in the visible and near-infrared region. Average absorption of thin films made of crumpled graphene balls can reach up to 97.4% in the wavelength region of 350-2500 nm. When crumpled graphene balls are used as the solar absorber for the interfacial evaporation system, evaporation efficiency of 84.6% was obtained under one sun at ambient pressure. Enhanced solar absorption of crumpled graphene balls, coupled with their aggregation-resistance and universal solution processability makes them promising candidates for solar heating/distillation applications.

Introduction

Efficient utilization of solar energy has attracted significant interest in society due to continuously increasing energy demand and depleting fossil fuel resources. To enhance the efficiency of solar absorption and convert the solar energy into other forms of energy such as thermal,[1-3] electrical,[4-6] and chemical energy,[7-9] carbon-based materials, including fullerenes[10,11] and vertically aligned carbon nanotubes,[12,13] have been previously studied as broadband solar absorbers. In recent years, graphene-based sheets have attracted significant interest as a promising photothermal harvester of solar energy.[14-16] Perfect monolayer of graphene can absorb ~2.3% incident light in the visible range.[17] Reduced graphene oxide (r-GO),[18-20] as a more scalable alternative to graphene made by mechanical exfoliation or chemical vapor deposition, has also been studied and achieved average broadband absorption around 85%.[21] The relatively high reflection (~15%) due to the stacking of multiple r-GO layers[22] in their thin film forms, however, has limited their performance as broadband absorber. There have been recent efforts in improving the optical absorption of graphene based films.[21,23-25] Qu *et al.*[26] fabricated vertically aligned graphene sheet membrane through antifreeze-assisted freezing approach and enabled the broadband absorption of the graphene film.

In this work, we studied the light harvesting capability of films of crumpled graphene balls (CGBs), which are sub-micron sized r-GO particles with paper ball-like morphology.[27] These particles have rough outer and inner surface at a length scale well below sub-microns, leading to high broadband absorption over 97% from visible (VIS) to near-infrared (NIR) region. They are also aggregation-resistant[28-30] and will not stack to form highly reflective microstructures, even after densification. Our earlier studies have found that wrinkles and folds in r-GO thin films cause strong light scattering.[31] Due to their crumpled paper ball-like structure, CGBs could better trap incident light by scattering both between the neighboring CGBs as well as inside the individual particles, which is full of wrinkled and folded domains of r-GO (Figure 1a). This greatly increases the optical path within the CGB films and leads to more efficient light absorption. With relatively simple generation process and the enhanced optical absorption, CGB films will help expand the application of graphene-based materials as broadband solar absorbers. The combination of high light absorption, high specific surface area, and thermal stability makes the CGB film an effective photothermal conversion layer in the interfacial evaporation system.

Experimental

Materials and Methods

[a] State Key Laboratory of Metal Matrix Composites, School of Materials Science and Engineering, Shanghai Jiao Tong University, 800 Dong Chuan Road, Shanghai 200240, P.R.China
[b] Department of Materials Science and Engineering, Northwestern University, 2220 Campus Drive, Evanston, IL 60208, USA

† Electronic Supplementary Information (ESI) available: SEM images and size distributions of CGB films; Reflection and transmission spectra of r-GO and CGB films; Reflection spectra of PTFE filter; Simulation reflection distribution of the upper surface of CGB800 film under one sun at different illuminating wavelength; Contact angle of CGB800 film and r-GO film; Evaporation mass changes using r-GO and CGB films. See DOI: 10.1039/x0xx00000x

All chemical reagents were purchased from Sinopharm Chemical Reagent Co., Ltd., without further purification.

Synthesis and Purification of Graphene Oxide

Graphite oxide (GO) was pre-oxidized and synthesized by a modified Hummers method[32] and purified by a two-step washing method. 50 mL concentrated H_2SO_4 was added in a 250-mL round-bottom flask and heated to 80 °C. 10 g $K_2S_2O_8$ and 10 g P_2O_5 were added in the H_2SO_4 and the solution was stirred until the solutes dissolved. 12 g graphite powder (Bay Carbon Inc., SP-1 grade) was added into the mixture and stirred for 4.5 h at 80 °C. The pre-oxidized graphite powder solution was cooled down to room temperature, diluted with 100-mL deionized (DI) water, filtered with PTFE membrane (Millipore) and then rinsed with DI water to remove the residual reagents. The pre-oxidized graphite powder was then dried in air over night and collected for further oxidization.

The pre-oxidized graphite powder was stirred in a 2-L Erlenmeyer flask with 460-mL concentrated H_2SO_4 and kept at 0 °C in an ice bath. 60 g $KMnO_4$ was gradually added into the flask while the temperature was controlled at 0 °C. After adding $KMnO_4$, the flask was moved to a water bath of 35 °C for 2 h to complete oxidation. The flask was then transferred to the ice bath again and 1-L DI water was slowly added into the mixture to dilute the H_2SO_4 solution. After dilution, 50-mL 30 wt% H_2O_2 was added dropwise into the flask to reduce the remaining oxidant. The mixture was filtered with PTFE membrane (Millipore) and rinsed with aqueous HCl solution (3.4%) to remove the residual reagents. The mixture was then re-dispersed in acetone, filtered again with PTFE membrane (Millipore), and rinsed with acetone to remove the residual HCl. The obtained GO was collected, dried in air, and then stored for future usage.

Synthesis of Crumpled Graphene Balls

Crumpled graphene balls (CGBs) were prepared using capillary compression through rapid evaporating of GO sheet aerosol droplets reported previously.[27] The as-prepared GO sheets were dispersed in water at a concentration of 1.0 mg mL^{-1} by an ultrasonic cleaner (40kHz, KQ5200DE, Kunshan Ultrasonic Instruments Co., LTD). Aerosol droplets of GO sheets, generated by a ultrasonic atomizer (1.7 MHz, SS-6B, Shuangsheng Medical Co., LTD), were carried by nitrogen gas (1L min^{-1}) through a tube furnace (SLG1400-60, Shanghai Shengli Test Instruments CO.,LTD; tube diameter = 25 mm) that was preheated to 500 °C. A PTFE filter (Hydrophilic, pore size: 100nm, Haiyan New Oriental Plastify Technology Co., LTD) was placed at the end of the tube furnace to collect the partially reduced CGBs (CGB500). The CGB500 were collected into a quartz boat and further annealed at 600 °C, 700 °C and 800 °C in tube furnace under nitrogen atmosphere for 2 h.

Preparation of CGB Thin Film

The as-prepared CGBs were re-dispersed in ethanol with a concentration of 0.1 mg mL^{-1} by using the ultrasonic cleaner. Then the mixture was filtered with a PTFE filter to obtain CGB thin films with area densities of around 1.0 mg cm^{-2}. The CGB/PTFE composite membranes were cut to circles with diameter of 1.68 cm and stored for further steam-generation experiment.

Synthesis of Reduced-Graphene Oxide Thin Film

Reduced graphene oxide (r-GO) was prepared in a hydrothermal process. 15-ml GO solution (0.1 mg mL^{-1}) was mixed with 15-mL ethanol in the hydrothermal reactor and heated in oven (LS-VO20, Labserv Ltd) at 120 °C for 15 h. The generated r-GO solution was further dried in a freeze dryer (FD-1A-50, Beijing Boyikang Laboratory Instruments Co., Ltd) for 24 h to avoid regraphitization. The r-GO was collected and the r-GO/PTFE composite membrane was prepared using the same process as used in preparing the CGB/PTFE composite membrane.

Characterization and Property Measurement

Scanning electron microscope (SEM; 5 kV, Sirion 200 from FEI) was used in these experiments to characterize the microstructure of the thin films. X-ray photoelectron spectroscopy (XPS; Kratos AXIS Ultra) was used to characterize the chemical composition of the r-GO and CGB samples. Ultraviolet-visible-NIR spectrophotometer equipped with an integrating sphere (Lambda 750S, PerkinElmer Inc.) was used to measure the hemisphere reflection and transmission of the thin films. Contact angle was measured by contact angle meter (DSA30, KRUSS GmbH, Germany).

Evaporation Performance Measurement

Xenon light (BILON-GHX-Xe-300, Shanghai Binlon Instrument Co., LTD), which has a similar output spectrum as the sun simulator, was used as light source and the light intensity was measured by a power meter (CEL-NP2000, Ceaulight Co. LTD). Weight of the evaporation system was measured by an electronic balance (BSM-220.4, Zhuojing Electronic Technology Co., LTD). An IR camera (T620, FLIR Systems Inc.) was used in the temperature measurement during the evaporation process. The background water evaporation rate was measured without the solar absorber films (CGB and r-GO films). The background rate was measured to be 0.4866 Kg m^{-2} h^{-1}.

Results and discussion

CGBs were synthesized by an aerosol assisted capillary compression process as illustrated in Figure 1b.[27] First, aerosol droplets of graphene oxide (GO) sheets were created by an ultrasonic nebulizer and passed through a tube furnace pre-heated at 500 °C. The capillary force generated by the evaporating liquid droplets compressed the GO sheets into crumpled paper ball shape. During the flight through the heated furnace, GO also became partially reduced, which is reflected in the dark brown to black color of the collected powders. To further reduce the as-prepared samples (Figure 1c), the CGBs collected at 500°C were further annealed at 600

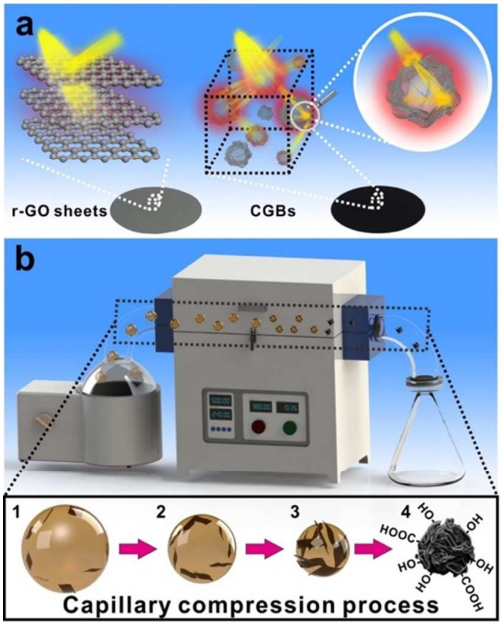

Figure 1. (a) Schematic drawings illustrating that flake-like graphene layers become reflective due to their planar microstructure, while layers of crumpled graphene balls are non-reflective due to extensive scattering within or between the particles. (b) Drawings illustrating the aerosol-assisted capillary compression route to synthesize CGBs.

°C, 700 °C and 800 °C, and the corresponding samples are named CGB500, CGB600, CGB700 and CGB800, respectively.

Powders of crumpled graphene balls are then dispersed in water and deposited on polytetrafluoroethylene (PTFE) filter membrane by filtration (Figure 2a) to create CGB/PTFE bilayer films for interfacial evaporation studies. A control sample of r-GO sheets was prepared by the same method as CGB film. The photo in Figure 2b shows the r-GO sheets and CGB500 films, both of which were made with similar area densities of around 1.0 mg cm^{-2}. Figure 2c-2d are scanning electron microscopy (SEM) images of the CGB500 film, showing that the CGBs are indeed closely packed but not aggregated. The average diameter of the particles was found to be around 400 nm. Compared with r-GO, the crumpling structure is quite stable and it does not unfold or collapse during annealing.[27] In deed, additional SEM studies confirmed similar size distribution and morphology for the other CGB samples (Figure S1). Figure 2e-2f shows the microstructure of the r-GO sheet. Without the crumpled structure, the paralleled flat r-GO layers stack with each other and form a lamellar film. Although the CGB500 sample were less reduced than the r-GO sheets (see Figure 3 for XPS analysis), its film appears much darker than the one made of r-GO sheets, which suggests that the crumpled structures indeed significantly reduce light reflection.

The volume densities of CGB800 film and the r-GO film are calculated based on their thicknesses measured in cross-sectional SEM imaging. With the same area density of 1.0 mg cm^{-2}, and the thickness of 78.9 μm and 56.0 μm, the volume densities of the CGB800 and r-GO films were calculated to be 0.127 g cm^{-3} and 0.179 g cm^{-3}, respectively. The CGB film has lower volume density since there are tens of nanometer sized

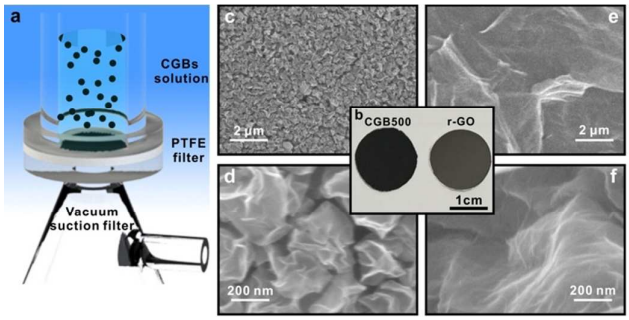

Figure 2. (a) Schematic drawing showing the filtration process used to prepare thin films of r-GO and CGBs. (b) Photos of CGB500 and r-GO sheet deposited on a PTFE filter membrane with the same loading level of 1.0 mg cm^{-2}. Although the level of oxidation of CGB500 sample is found to be higher than the r-GO sheets, its film appears a lot darker, which is attributed to its much stronger light scattering capability of the crumpled microstructures. Indeed, SEM images of the CGB500 sample (c, d) show uniform distribution of heavily crumpled features at sub-micron length scale throughout the film. In contrast, the r-GO film is much more reflective due to its smoother microstructures (e, f).

voids inside and between each crumpled particles. As shown in Figure S7, CGB800 film has a much larger porosity (~1.14 $cm^3 g^{-1}$) than that of the r-GO film (~0.17 $cm^3 g^{-1}$).

X-ray photoelectron spectroscopy (XPS) was used to confirm the chemical composition of the r-GO and CGB samples annealed at different temperatures (Figure 3). The atomic percentage of oxygen in GO was found to be around 28.3%, and decreased slightly to 23.7% after passing through the tube furnace (CGB500). This small degree of reduction is attributed to very short time-of-flight of the flowing aerosol droplets, which does not allow sufficient heating of the crumpled particles. After further annealing, the oxygen content of CGB600, CGB700 and CGB800 decreased to 11.9%, 10.5% and 7.2%, respectively. The oxygen content of the r-GO sheets was 19.7%. The XPS spectrum of the C 1s for CGB800 (Figure 3g) has three peaks at 284.1, 285.0, and 289.1 eV, which can be assigned to C-C/C=C, C-O and C=O groups, respectively.[33] Compared with GO (Figure 3b), the amount of C-O bond in the CGB800 decreases substantially and the amount of C=O bond decreases only slightly. Such change indicates that the quantity of the hydroxyl and epoxy groups on the graphene layer decreases significantly, accompanying with the recovery the π conjugation network on the basal plane of r-GO.

The reflection and transmission of the r-GO and CGB films in the wavelength region of 350-2500 nm were measured using an integrating sphere (Figure S2). The absorption of all thin films
can be calculated by equation 1:

$$\boldsymbol{A} = 1 - \boldsymbol{R} - \boldsymbol{T} \quad (1),$$

where $\boldsymbol{A}$ represents absorption, $\boldsymbol{R}$ reflection and $\boldsymbol{T}$ the transmission. The average absorption for all the CGB thin films was above 95% (Figure 4a). From CGB500, CGB600, CGB700 to CGB800, the average absorption of their thin films are 96.3%, 96.8%, 97.4%, and 97.4%, respectively, all of which are significantly larger than that of the r-GO film (84.3%). Figure 4b shows the specular reflection of the CGB800 film in the mid-IR

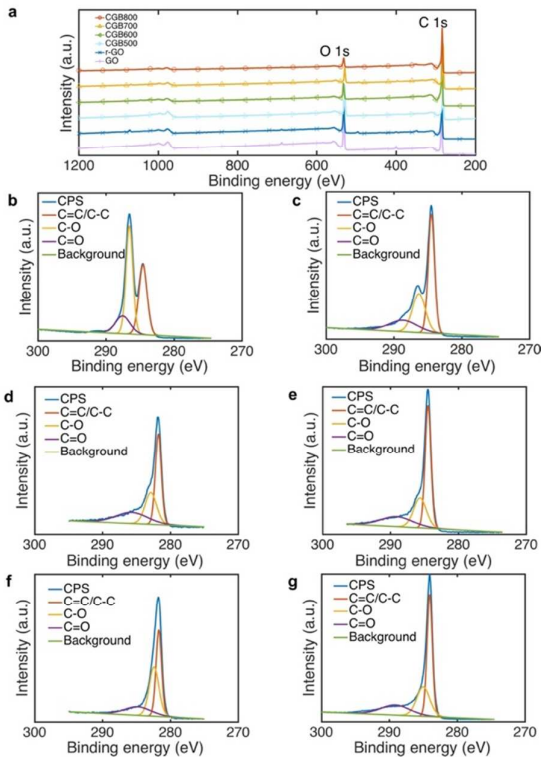

Figure 3. (a) XPS spectrum of GO, r-GO and CGB samples. XPS spectra of C 1s for (b) GO, (c) r-GO, (d) CGB500, (e) CGB600, (f) CGB700, and (g) CGB800.

region of 2.5-14.8 μm, which is measured to be around only 0.20 %.

The light absorption of these graphene-based materials was mainly influenced by two factors: microstructure and oxygen content of the graphene layers. The crumpled structure of CGBs successfully prevented the stacking of the graphene layers, thus reduced the reflection due to stacked structures with more than 10 layers of graphene.[22] Beside reduced reflection, light illuminating the surface CGB films is also heavily scattered due to the rough outer and inner surface of each crumpled particles at a length scale well below sub-microns. Reduced reflection and the multi-scattering mechanism leads to the excellent light absorption properties of CGBs. Annealing CGBs at higher temperatures helps remove more oxygen-containing functional groups and increase the degree of π conjugation, making them absorb light even more strongly.[34]

We also calculated the optical properties of CGB films through theoretical simulation based on the single particle Mie scattering model.[35] TracePro software was used to build the model of the closed packed CGB film with detailed descriptions provided in the supporting information. In the simulation, two detectors were placed at the upper and lower surfaces of the CGB800 film to collect the reflection and transmission of the light. Figure 4c shows the simulated reflection of CGB800 film in the wavelength range of 250 to 2500 nm. The insets are the simulated reflection distributions of CGB800 film under one sun at wavelengths of 500nm, 1250nm and 2000nm. With increasing wavelength, simulated reflection of the CGB800 film

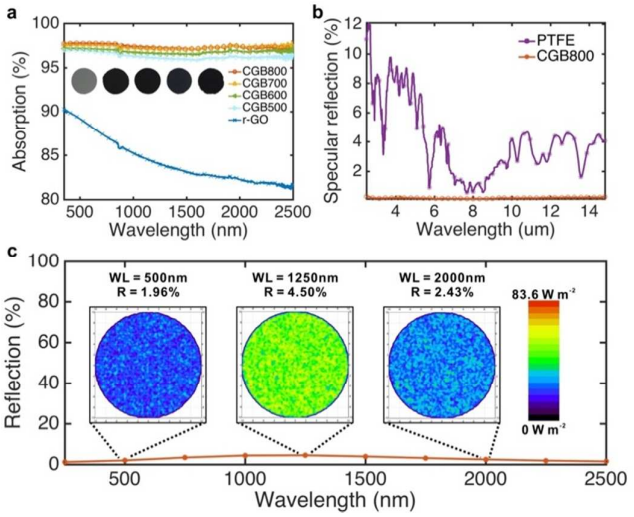

Figure 4. (a) UV-VIS-NIR absorption spectra of r-GO and CGB thin films. The inset shows the optical image of r-GO, CGB500, CGB600, CGB700 and CGB800 thin films from left to right. (b) Specular reflection of CGB800 (red) and PTFE (purple) in Mid-IR region. (c) Simulated reflectance of CGB800 film under illumination at different wavelengths. The insets show the simulated reflection distribution of the upper surface of the CGB thin film under one sun at illuminating wavelength of 500 nm, 1250 nm and 2000 nm. The color scale on the right shows the level of light intensity in reflection.

increases from 1.2% at 250 nm to 4.5% at 1250 nm, and then decreases to 1.5% at 2500 nm. The transmission is near zero at all wavelengths in this range. The simulated result deviated marginally from our experimental data, because only the first order of the multi-scattering was used in the calculation. The use of uniform sphere balls with close packing to represent the crumpled shape of CGBs may also contribute to the difference between the simulation and the experiments.

Next, CGB films are integrated into a solar driven interfacial evaporation system. The self-floating interfacial evaporation system was fabricated by placing the CGB/PTFE membrane on top of a piece of expandable polyethylene (EPE) foam wrapped by a piece of air-laid paper (Figure 5a). The CGB layer served as the light to heat conversion layer. With the low thermal conductivity of EPE foam (~0.032 W m^{-1} K^{-1})[36] and high water replenishment speed of the air-laid paper, the multi-layered system can efficiently harvest solar energy for rapid evaporation at the liquid-air interface. The converted heat is localized at the interface, which leads to evaporation efficiencies greater than those of conventional bulk heating approaches.[37-40] For effective transfer of solar generated heat to water, these CGBs need to display good wettability. Upon contact between water and CGB films generated in this work, the contact angles of water gradually decreased from ~10° to 0° in about 5s (Figure S4 and Movie S1). The numerous pores between CGBs form an interconnected 3D network that absorbs the water droplet into the CGB film. During the evaporation process, this 3D network also helps replenish water at the top surface of CGBs through capillary wicking. The mass change of water during the evaporation process was recorded by an analytical balance (Figure S5). The evaporation rate at the equilibrium state was calculated based on the slope

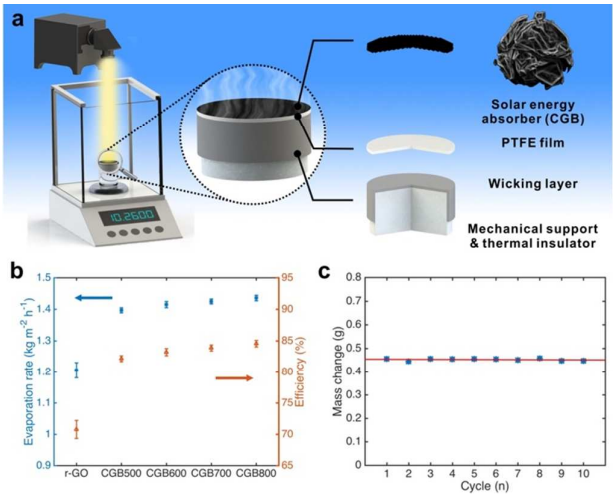

Figure 5. (a) Drawing illustrating the experimental setup for interfacial evaporation study. (b) Evaporation rate and efficiency of r-GO and CGB films. (c) The mass change of evaporation after 0.5 h using the same CGB800 film for 10 cycles.

of the mass change curve. Figure 5b shows that after subtracting background evaporation, the evaporation rate of the CGB800 reached 1.436 kg m^{-2} h^{-1}. Under the same conditions, the evaporation rates of r-GO, CGB500, CGB600, and CGB700 were 1.206, 1.397, 1.415 and 1.425 kg m^{-2} h^{-1}, respectively. All evaporation rates of the CGB films were larger than that of the r-GO film due to the greater light absorption of the CGB films than that of the r-GO film.

The evaporation efficiency was calculated using equation 2:

$$\eta = \frac{\dot{m}H_{LV}}{C_{opt}P} \quad (2),$$

where $\dot{m}$ is the mass flux of vapor, H_{LV} is the total enthalpy change during the evaporation process, C_{opt} is the optical concentration, and P is the nominal power density of solar illumination. Figure 5b shows the calculated evaporation efficiencies. The evaporation efficiency of CGB800 reached 84.6% under one sun, which is among the best reported in the literature for graphene-based systems. CGB500, CGB600, and CGB700 samples also attained efficiencies of 82.2%, 83.2%, and 83.9%, respectively. The evaporation efficiency of the r-GO film was 70.8%, which was similar to the values reported by others.[41] As a demonstration of device stability, interfacial evaporation experiments were repeated ten times using the same CGB800 film. Mass change of water after 0.5 h for each repetition were showed in Figure 5c, where the average mass change of the ten cycles was 0.452 ± 0.004 g. Figure S8 also shows that the microstructure of the CGB800 film remained the same after the cycling.

Conclusions

This work demonstrates that CGBs are highly efficient broadband solar absorbers due to their unique morphology and aggregation-resistant properties. The crumpled paper ball-like structure of r-GO greatly reduces the surface reflection in their thin film forms, leading to significantly higher light absorption than the sheet-like r-GO. Consistently strong light absorption larger than 96% in the wavelength range of 350-2500 nm was achieved for CGBs annealed between 500-800 °C. The strong broadband light absorption capability of CGBs was employed for making interfacial solar evaporation systems, which delivered efficiencies of around 84.6% under one sun at ambient pressure. The combination of strong light absorption capability and thermal stability makes crumpled graphene balls an attractive candidate for a number of solar-enabled applications, including solar distillation, solar thermal power generation, and thermal energy storage.

Conflicts of interest

There are no conflicts to declare.

Acknowledgements

T.D. thanks the financial support from National Key R&D Program of China (No. 2017YFB0406100), National Natural Science Foundation of China (Grant No: 21401129, 51521004, 51420105009 and 51403127), Natural Science Foundation of Shanghai (Grant No: 14ZR1423300), the Zhi-Yuan Endowed fund from Shanghai Jiao Tong University. J.H. thanks the support from the Office of Naval Research in the US (ONR-N000141310556 and then N000141612838). K.C. thanks the National Science Foundation for Graduate Research Fellowship.

Notes and references

1. Tian, B.; Wang, C.; Zhang, S.; Feng, L. Z.; Liu, Z. Photothermally Enhanced Photodynamic Therapy Delivered by Nano-Graphene Oxide. *Acs Nano* **2011,** *5*, 7000.
2. Ito, Y.; Tanabe, Y.; Han, J. H.; Fujita, T.; Tanigaki, K.; Chen, M. W. Multifunctional Porous Graphene for High-Efficiency Steam Generation by Heat Localization. *Adv. Mater.* **2015,** *27*, 4302.
3. Loomis, J.; Fan, X. M.; Khosravi, F.; Xu, P.; Fletcher, M.; Cohn, R. W.; Panchapakesan, B. Graphene/elastomer composite-based photo-thermal nanopositioners. *Sci. Rep.* **2013,** *3,* 1900.
4. Koppens, F. H. L.; Mueller, T.; Avouris, P.; Ferrari, A. C.; Vitiello, M. S.; Polini, M. Photodetectors based on graphene, other two-dimensional materials and hybrid systems. *Nat. Nanotechnol.* **2014,** *9*, 780.
5. Yan, K.; Wu, D.; Peng, H. L.; Jin, L.; Fu, Q.; Bao, X. H.; Liu, Z. F. Modulation-doped growth of mosaic graphene with single-crystalline p-n junctions for efficient photocurrent generation. *Nat. Commun.* **2012,** *3, 1280*.
6. Moghaddam, M. V.; Yaghoobi, P.; Sawatzky, G. A.; Nojeh, A. Photon-Impenetrable, Electron-Permeable: The Carbon Nanotube Forest as a Medium for Multiphoton Thermal-Photoemission. *Acs Nano* **2015,** *9*, 4064.
7. Park, J. H.; Kim, S.; Bard, A. J. Novel carbon-doped TiO2 nanotube arrays with high aspect ratios for efficient solar water splitting. *Nano Lett.* **2006,** *6*, 24.
8. Lara-Avila, S.; Moth-Poulsen, K.; Yakimova, R.; Bjornholm, T.; Fal'ko, V.; Tzalenchuk, A.; Kubatkin, S. Non-Volatile Photochemical Gating of an Epitaxial Graphene/Polymer Heterostructure. *Adv. Mater.* **2011,** *23*, 878.

9. Li, Q.; Guo, B. D.; Yu, J. G.; Ran, J. R.; Zhang, B. H.; Yan, H. J.; Gong, J. R. Highly Efficient Visible-Light-Driven Photocatalytic Hydrogen Production of CdS-Cluster-Decorated Graphene Nanosheets. *J. Am. Chem. Soc.* **2011,** *133*, 10878.
10. Shen, Y. F.; Skirtach, A. G.; Seki, T.; Yagai, S.; Li, H. G.; Mohwald, H.; Nakanishi, T. Assembly of Fullerene-Carbon Nanotubes: Temperature Indicator for Photothermal Conversion. *J. Am. Chem. Soc.* **2010,** *132*, 8566.
11. Thompson, B. C.; Frechet, J. M. J. Organic photovoltaics - Polymer-fullerene composite solar cells. *Angew. Chem. Int. Ed.* **2008,** *47*, 58.
12. Mizuno, K.; Ishii, J.; Kishida, H.; Hayamizu, Y.; Yasuda, S.; Futaba, D. N.; Yumura, M.; Hata, K. A black body absorber from vertically aligned single-walled carbon nanotubes. *P. Natl. Acad. Sci.* **2009,** *106*, 6044.
13. Nemilentsau, A. M.; Rotkin, S. V. Vertical Single-Wall Carbon Nanotube Forests as Plasmonic Heat Pipes. *Acs Nano* **2012,** *6*, 4298.
14. Ghasemi, H.; Ni, G.; Marconnet, A. M.; Loomis, J.; Yerci, S.; Miljkovic, N.; Chen, G. Solar steam generation by heat localization. *Nat. Commun.* **2014,** *5,* 5449.
15. Zhu, M. W.; Li, Y. J.; Chen, G.; Jiang, F.; Yang, Z.; Luo, X. G.; Wang, Y. B.; Lacey, S. D.; Dai, J. Q.; Wang, C. W.; Jia, C.; Wan, J. Y.; Yao, Y. G.; Gong, A.; Yang, B.; Yu, Z. F.; Das, S.; Hu, L. B. Tree-Inspired Design for High-Efficiency Water Extraction. *Adv. Mater.* **2017,** *29*. DOI: 10.1002/adma.201704107.
16. Li, Y. J.; Gao, T. T.; Yang, Z.; Chen, C. J.; Kuang, Y. D.; Song, J. W.; Jia, C.; Hitz, E. M.; Yang, B.; Hu, L. B. Graphene oxide-based evaporator with one-dimensional water transport enabling high-efficiency solar desalination. *Nano Energy* **2017,** *41*, 201.
17. Nair, R. R.; Blake, P.; Grigorenko, A. N.; Novoselov, K. S.; Booth, T. J.; Stauber, T.; Peres, N. M. R.; Geim, A. K. Fine structure constant defines visual transparency of graphene. *Science* **2008,** *320*, 1308.
18. Eda, G.; Chhowalla, M. Chemically Derived Graphene Oxide: Towards Large-Area Thin-Film Electronics and Optoelectronics. *Adv. Mater.* **2010,** *22*, 2392.
19. Zhu, Y. W.; Murali, S.; Cai, W. W.; Li, X. S.; Suk, J. W.; Potts, J. R.; Ruoff, R. S. Graphene and Graphene Oxide: Synthesis, Properties, and Applications. *Adv. Mater.* **2010,** *22*, 5226.
20. Li, D.; Kaner, R. Extending polymer conjugation into the second dimension. *Science* **2008,** *320*, 10.1126.
21. Hu, X. Z.; Xu, W. C.; Zhou, L.; Tan, Y. L.; Wang, Y.; Zhu, S. N.; Zhu, J. Tailoring Graphene Oxide-Based Aerogels for Efficient Solar Steam Generation under One Sun. *Adv. Mater.* **2017,** *29*. DOI: 10.1002/adma.201604031.
22. Casiraghi, C.; Hartschuh, A.; Lidorikis, E.; Qian, H.; Harutyunyan, H.; Gokus, T.; Novoselov, K. S.; Ferrari, A. C. Rayleigh imaging of graphene and graphene layers. *Nano Lett.* **2007,** *7*, 2711.
23. Li, Y. J.; Gao, T. T.; Yang, Z.; Chen, C. J.; Luo, W.; Song, J. W.; Hitz, E.; Jia, C.; Zhou, Y. B.; Liu, B. Y.; Yang, B.; Hu, L. B. 3D-Printed, All-in-One Evaporator for High-Efficiency Solar Steam Generation under 1 Sun Illumination. *Adv. Mater.* **2017,** *29*. DOI: 10.1002/adma.201700981.
24. Shi, L.; Wang, Y. C.; Zhang, L. B.; Wang, P. Rational design of a bi-layered reduced graphene oxide film on polystyrene foam for solar-driven interfacial water evaporation. *J. Mater. Chem. A* **2017,** *5,* 16212.
25. Ren, H. Y.; Tang, M.; Guan, B. L.; Wang, K. X.; Yang, J. W.; Wang, F. F.; Wang, M. Z.; Shan, J. Y.; Chen, Z. L.; Wei, D.; Peng, H. L.; Liu, Z. F. Hierarchical Graphene Foam for Efficient Omnidirectional Solar-Thermal Energy Conversion. *Adv. Mater.* **2017,** *29*. DOI: 10.1002/adma.201702590.
26. Zhang, P. P.; Li, J.; Lv, L. X.; Zhao, Y.; Qu, L. T. Vertically Aligned Graphene Sheets Membrane for Highly Efficient Solar Thermal Generation of Clean Water. *Acs Nano* **2017,** *11*, 5087.
27. Luo, J. Y.; Jang, H. D.; Sun, T.; Xiao, L.; He, Z.; Katsoulidis, A. P.; Kanatzidis, M. G.; Gibson, J. M.; Huang, J. X. Compression and Aggregation-Resistant Particles of Crumpled Soft Sheets. *ACS Nano* **2011,** *5*, 8943.
28. Luo, J. Y.; Jang, H. D.; Huang, J. X. Effect of Sheet Morphology on the Scalability of Graphene-Based Ultracapacitors. *Acs Nano* **2013,** *7*, 1464.
29. Luo, J. Y.; Kim, J.; Huang, J. X. Material Processing of Chemically Modified Graphene: Some Challenges and Solutions. *Acc. Chem. Res.* **2013,** *46*, 2225.
30. Dou, X.; Koltonow, A. R.; He, X. L.; Jang, H. D.; Wang, Q.; Chung, Y. W.; Huang, J. X. Self-dispersed crumpled graphene balls in oil for friction and wear reduction. *P. Natl. Acad. Sci.* **2016,** *113*, 1528.
31. Cote, L. J.; Kim, J.; Zhang, Z.; Sun, C.; Huang, J. X. Tunable assembly of graphene oxide surfactant sheets: wrinkles, overlaps and impacts on thin film properties. *Soft Matter* **2010,** *6*, 6096.
32. Kim, F.; Luo, J. Y.; Cruz-Silva, R.; Cote, L. J.; Sohn, K.; Huang, J. X. Self-Propagating Domino-like Reactions in Oxidized Graphite. *Adv. Funct. Mater.* **2010,** *20*, 2867.
33. Stankovich, S.; Dikin, D. A.; Piner, R. D.; Kohlhaas, K. A.; Kleinhammes, A.; Jia, Y.; Wu, Y.; Nguyen, S. T.; Ruoff, R. S. Synthesis of graphene-based nanosheets via chemical reduction of exfoliated graphite oxide. *Carbon* **2007,** *45*, 1558.
34. Robinson, J. T.; Tabakman, S. M.; Liang, Y. Y.; Wang, H. L.; Casalongue, H. S.; Vinh, D.; Dai, H. J. Ultrasmall Reduced Graphene Oxide with High Near-Infrared Absorbance for Photothermal Therapy. *J. Am. Chem. Soc.* **2011,** *133*, 6825.
35. Heinisch, R. L.; Bronold, F. X.; Fehske, H. Mie scattering analog in graphene: Lensing, particle confinement, and depletion of Klein tunneling. *Phys. Rev. B* **2013,** *87,* 155409.
36. Almanza, O.; Rodriguez-Perez, M. A.; De Saja, J. A. Applicability of the transient plane source method to measure the thermal conductivity of low-density polyethylene foams. *J. Polym. Sci., Part B: Polym. Phys.* **2004,** *42*, 1226.
37. Liu, Y. M.; Yu, S. T.; Feng, R.; Bernard, A.; Liu, Y.; Zhang, Y.; Duan, H. Z.; Shang, W.; Tao, P.; Song, C. Y.; Deng, T. A Bioinspired, Reusable, Paper-Based System for High-Performance Large-Scale Evaporation. *Adv. Mater.* **2015,** *27*, 2768.
38. Zhou, L.; Tan, Y. L.; Wang, J. Y.; Xu, W. C.; Yuan, Y.; Cai, W. S.; Zhu, S. N.; Zhu, J. 3D self-assembly of aluminium nanoparticles for plasmon-enhanced solar desalination. *Nat. Photonics* **2016,** *10*, 393.
39. Li, X. Q.; Xu, W. C.; Tang, M. Y.; Zhou, L.; Zhu, B.; Zhu, S. N.; Zhu, J. Graphene oxide-based efficient and scalable solar desalination under one sun with a confined 2D water path. *P. Natl. Acad. Sci.* **2016,** *113*, 13953.
40. Xu, N.; Hu, X. Z.; Xu, W. C.; Li, X. Q.; Zhou, L.; Zhu, S. N.; Zhu, J. Mushrooms as Efficient Solar Steam-Generation Devices. *Adv. Mater.* **2017,** *29*. DOI: 10.1002/adma.201606762.
41. Wang, G.; Fu, Y.; Ma, X. F.; Pi, W. B.; Liu, D. W.; Wang, X. B. Reusable reduced graphene oxide based double-layer system modified by polyethylenimine for solar steam generation. *Carbon* **2017,** *114*, 117.

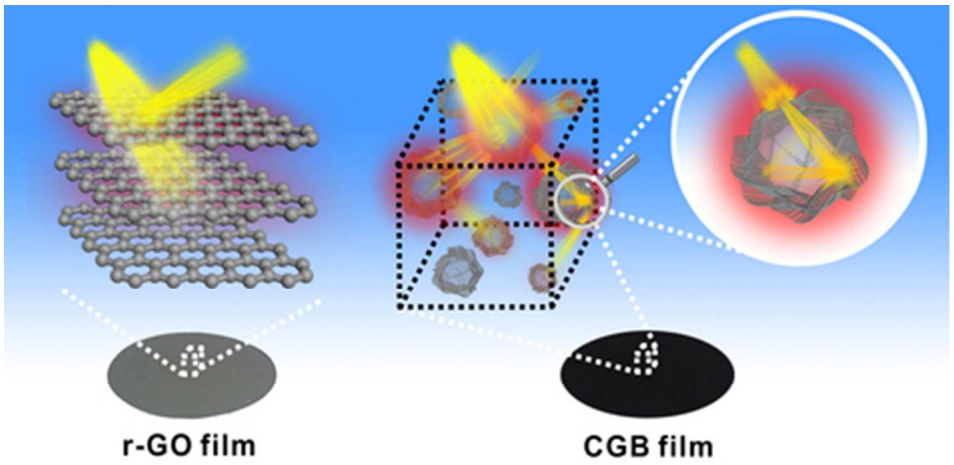

Crumpled microstructures enable reduction of reflection at the graphene surface and make crumpled graphene balls as excellent broadband light absorbers.

39x19mm (300 x 300 DPI)